ORIGINAL ARTICLE

^{18}F-fluoromisonidazole positron emission tomography can predict pathological necrosis of brain tumors

Takuya Toyonaga[1] · Kenji Hirata[1] · Shigeru Yamaguchi[1,2] · Kanako C. Hatanaka[3] ·
Sayaka Yuzawa[4] · Osamu Manabe[1] · Kentaro Kobayashi[1] · Shiro Watanabe[1] ·
Tohru Shiga[1] · Shunsuke Terasaka[2] · Hiroyuki Kobayashi[2] · Yuji Kuge[5] ·
Nagara Tamaki[1]

Abstract

Purpose Tumor necrosis is one of the indicators of tumor aggressiveness. ^{18}F-fluoromisonidazole (FMISO) is the most widely used positron emission tomography (PET) tracer to evaluate severe hypoxia in vivo. Because severe hypoxia causes necrosis, we hypothesized that intratumoral necrosis can be detected by FMISO PET in brain tumors regardless of their histopathology. We applied FMISO PET to various types of brain tumors before tumor resection and evaluated the correlation between histopathological necrosis and FMISO uptake.

Methods This study included 59 brain tumor patients who underwent FMISO PET/computed tomography before any treatments. According to the pathological diagnosis, the brain tumors were divided into three groups: astrocytomas (group 1), neuroepithelial tumors except for astrocytomas (group 2), and others (group 3). Two experienced neuropathologists evaluated the presence of necrosis in consensus. FMISO uptake in the tumor was evaluated visually and semi-quantitatively using the tumor-to-normal cerebellum ratio (TNR).

Results In visual analyses, 26/27 cases in the FMISO-positive group presented with necrosis, whereas 28/32 cases in the FMISO-negative group did not show necrosis. Mean TNRs with and without necrosis were 3.49 ± 0.97 and 1.43 ± 0.42 ($p < 0.00001$) in group 1, 2.91 ± 0.83 and 1.44 ± 0.20 ($p < 0.005$) in group 2, and 2.63 ± 1.16 and 1.35 ± 0.23 ($p < 0.05$) in group 3, respectively. Using a cut-off value of TNR $= 1.67$, which was calculated by normal reference regions of interest, we could predict necrosis with sensitivity, specificity, and accuracy of 96.7, 93.1, and 94.9 %, respectively.

Conclusions FMISO uptake within the lesion indicated the presence of histological micro-necrosis. When we used a TNR of 1.67 as the cut-off value, intratumoral micro-necrosis was sufficiently predictable. Because the presence of necrosis implies a poor prognosis, our results suggest that FMISO PET could provide important information for treatment decisions or surgical strategies of any type of brain tumor.

✉ Shigeru Yamaguchi
yama-shu@med.hokudai.ac.jp

1 Department of Nuclear Medicine, Graduate School of Medicine, Hokkaido University, Kita 15, Nishi 7, Kita-Ku, Sapporo 060-8638, Japan

2 Department of Neurosurgery, Graduate School of Medicine, Hokkaido University, Sapporo, Japan

3 Department of Surgical Pathology, Hokkaido University Hospital, Sapporo, Japan

4 Department of Cancer Pathology, Graduate School of Medicine, Hokkaido University, Sapporo, Japan

5 Central Institute of Isotope Science, Hokkaido University, Sapporo, Japan

Introduction

Several subtypes of brain tumor develop intratumoral necrosis, and the presence of necrosis is usually an indicator of malignancy or a prognostic factor [1–4]. Tumor necrosis is well correlated with the mitotic index, increases in cellularity, and a high nucleus-to-cytoplasm ratio. These findings suggest

that necrosis might be correlated with tumor progression and therefore prognosis. Ring-like enhancement of contrast-enhanced computed tomography (CT) and magnetic resonance imaging (MRI) can detect macro-necrosis, but only histopathological examination can detect micro-necrosis. Tumor sampling is no doubt an important method to accurately evaluate tumor characteristics. In contrast, the invasiveness of tumor sampling is a clinical obstacle. Non-invasive prediction of the presence of necrosis would highly affect the treatment strategy.

In this study, we focused on the relationship between hypoxia and necrosis. Hypoxia is well known as a major factor in the induction of necrosis, which can be evaluated using ^{18}F-fluoromisonidazole (FMISO). FMISO is the most widely used positron emission tomography (PET) tracer to visualize severe hypoxia in vivo. It is a derivative of misonidazole (MISO) that is used as a radiosensitizer [5]. Mainly because of cytotoxicity, MISO has not been applied to treatment purposes [6]. Subsequently, FMISO was developed as a hypoxia imaging PET tracer [7, 8]. Several studies have suggested that FMISO accumulation may increase sharply under 10–20 mmHg of partial (p) O_2 [8, 9]. Piert et al. examined 14 pigs to evaluate liver tissue hypoxia induced by segmental arterial hepatic occlusion using dynamic PET scanning. Oxygen distributions were assessed directly by Eppendorf pO_2 measurements. They concluded that the decrease in pO_2 was associated with an increase in the FMISO standardized uptake value (SUV) under pO_2 below 20 mmHg [10, 11]. Bentzen et al. examined mice with mammary carcinoma using FMISO and Eppendorf pO_2 measurement. They reported that FMISO accumulation increased under a median pO_2 of 20 mmHg. In addition, they showed that higher inspired pO_2 reduced FMISO accumulation in the tumor [12].

We previously showed that FMISO accumulation distinguishes glioblastoma (GBM) from other lower-grade gliomas [13]. We hypothesized that FMISO PET could identify intratumoral necrosis not only in gliomas but also any type of brain tumor. To test this hypothesis, we applied FMISO PET to subjects with various types of brain tumors before tumor resection, and evaluated the correlation between histopathological necrosis and FMISO accumulation. We also evaluated the threshold of semi-quantitative values in these subjects, which might predict the presence of necrosis.

Materials and methods

Patients

This study included brain tumor patients who underwent FMISO PET or PET/CT before radiation therapy, chemotherapy, and surgical intervention. Patients who had not undergone tumor resection or biopsy after PET examinations were excluded. Overall, the study population included 59 patients (M:F = 33:26, age, 30–85 years). Surgeries were performed at Hokkaido University Hospital or our affiliated hospitals. Detailed surgical procedures are described below. Surgical specimens were collected by the Department of Pathology at Hokkaido University. The study was approved by the Ethics Committee of Hokkaido University Hospital (approval number 014–0381). Written informed consent was obtained from all patients.

Imaging protocol

All patients underwent MRI and FMISO PET or PET/CT before surgical intervention. MRI sequences included T1-weighted with and without gadolinium enhancement, T2-weighted, and fluid-attenuated inversion recovery (FLAIR) images. The types of MRI scanners depended on the facility.

For FMISO PET, patients were not asked to fast before the study. Static PET scanning was initiated at 4 h after intravenous injection of 400 MBq FMISO (406.42 ± 35.45 MBq) as recommended previously [14, 15]. PET scanners used in this study were an ECAT HR+ PET scanner (Asahi-Siemens Medical Technologies Ltd., Tokyo, Japan), Biograph 64 PET-CT scanner (Asahi-Siemens Medical Technologies Ltd., Tokyo, Japan), and Gemini TF64 TOF-PET/CT scanner (Hitachi Medical Corporation Ltd, Tokyo, Japan). All scanners were operated in the three-dimensional mode. For the ECAT HR+ scanner, the 10-min emission acquisition was followed by 3-min transmission scanning with a ^{68}Ge/^{68}Ga retractable line source. For the Biograph 64 PET/CT and Gemini TF PET/CT scanners, the 10-min emission acquisition was followed by CT scanning for attenuation correction. Attenuation-corrected radioactivity images were reconstructed using filtered back projection (ECAT and Biograph) or the ordered-subset expectation maximization method (Gemini) with a Hann filter of 4-mm full-width at half-maximum.

Visual analysis

Visual assessment of FMISO PET results has been described previously [13]. In this study, two nuclear medicine physicians (radiologist A: Ta.To. and radiologist B: Ke.Ko.) visually interpreted the FMISO PET images. Radiologists A and B have 2 and 6 years experience in PET/CT, respectively. They were blind to the clinical information and MRI results. According to FMISO accumulation, they categorized each image into three categories: low, intermediate, and high. For the final decision, the FMISO-positive group represented images that the two radiologists agreed were high FMISO uptake. In contrast, the FMISO-negative group represented images that either radiologist evaluated as low or intermediate uptake.

Semi-quantitative analysis

The tumor-to-normal cerebellum ratio (TNR) was calculated for semi-quantitative analysis. First, a nuclear medicine physician (Ta.To.) created 15 10-mm-diameter circular regions of interest (ROIs) (five ROIs on each of the axial slices) on both sides of the cerebellar cortex for a total of 30 ROIs per patient. The average values of these regions of the SUV were defined as normal references. The SUV was calculated as [tissue radioactivity (Bq/ml)] × [body weight(g)]/ [injected radioactivity(Bq)]. Second, we placed one 30-mm round volume of interest (VOI) containing the voxel of the tumor that showed the highest visual accumulation. The tumor regions were determined with reference to gadolinium-enhanced T1-weighted images. Then, the maximum SUV (SUVmax) of the tumor was divided by averaging the cerebellar SUV as the TNR. We adopted the mean + 3SD within cerebellar ROIs as the cut-off value for semi-quantitative analysis to avoid any influence of reconstruction noise, as established for whole-body [18]fluoro-2-deoxyglucose PET [16].

Surgical procedures

The detailed procedures of PET-guided surgery have been described previously [17]. In brief, all surgeries were performed using the Neuro-Navigation system (StealthStation®, Treon® or S7®, Medtronic). Before surgery, FMISO-uptake lesions were superimposed on T1-weighted images with gadolinium enhancement. When the patients underwent biopsy, the biopsy target was set in the FMISO-uptake lesion using the navigation system in cases of an identified FMISO uptake lesion. When the patients underwent maximum tumor resection, FMISO-accumulated areas were contained in the extent of resection as much as possible.

Pathological classification

According to the pathological diagnosis, brain tumors were divided into three groups: astrocytic tumors (group 1), neuroepithelial tumors other than astrocytic tumors (group 2), and other histopathological tumors (group 3). Group 1 included two diffuse astrocytomas (DAs), six anaplastic astrocytomas (AAs), and 17 GBMs. Group 2 included three oligoastrocytomas (OAs), one oligodendroglioma (OL), one central neurocytoma, one anaplastic ependymoma (AE), two anaplastic oligoastrocytomas (AOAs), eight anaplastic oligodendrogliomas (AOs), and five GBMs with an oligodendroglial component (GBMO). Group 3 included six primary central nerve system lymphomas (PCNSLs), two metastatic brain tumors, one craniopharyngioma, one hamartoma, one hemangioblastoma, one atypical meningioma, and one lymphomatoid granulomatosis (LYG) (Table 1).

Assessment of necrosis

Two experienced neuropathologists (Ka.Ha. and Sa.Yu.) assessed each specimen and evaluated the presence of necrosis in consensus. The diagnosis and evaluation were determined by agreement of the two pathologists.

Statistical analysis

All parametric variables are presented as the means ± SD. The weighted Kappa statistic was employed to evaluate interrater reproducibility of visual analyses. Mean values of the FMISO TNR were compared between groups by the Welch's t test. Fisher's exact test was employed to examine the relationship between the results of visual analyses and those of histopathological necrosis. The associations between image analysis and histopathological necrosis were examined by receiver operating characteristic (ROC) analysis. The cut-off value was represented within cerebellar ROIs. p values less than 0.05 were considered statistically significant. R 3.1.2 for Windows and the 'survival' package [18] were used for all statistical analyses.

Results

Histopathological necrosis and diagnosis

Histopathological necroses were observed in 17/17 GBMs (100 %), 5/5 GBMOs (100 %), 1/8 AOs (12.5 %), 1/1 AE (100 %), 4/6 PCNSLs (66.6 %), and 1/2 metastatic brain tumors (50 %), and 1/1 atypical meningioma (100 %). Necroses were found in 17/25 cases in group 1, 7/20 cases in group 2, and 6/14 cases in group 3.

Correlation between visual analysis and necrosis

Radiologist A evaluated 27/59 cases (45.8 %) as high uptake, 5/59 cases (8.5 %) as intermediate uptake, and 27/59 cases (45.8 %) as low uptake. Radiologist B rated 28/59 cases (47.5 %) as high uptake, 2/59 cases (3.4 %) as intermediate uptake, and 29/59 cases (49.2 %) as low uptake (Table 2). The weighted Kappa statistic of interrater reliability for FMISO uptake was very high ($k = 0.92$).

A total of 27/59 images, which were evaluated as high FMISO uptake by both radiologists, were categorized as FMISO-positive uptake lesions. A total of 32/59 images, which at least one radiologist evaluated as intermediate or low FMISO uptake, were categorized as FMISO-negative uptake lesions. The relationship between visual analysis and the presence of necrosis is summarized in Table 3. Fisher's exact test indicated a significant correlation between necrosis and

Table 1 Demographics of histopathological diagnosis

	All	Group 1	Group 2	Group 3
N	59	25	20	14
Age (range)	30–85	34–85	30–78	32–77
Sex (M:F)	33:26	8:16	13:7	10:4
Histopathological diagnosis (N)		DA (2)	OA (3)	PCNSL (6)
		AA (6)	OL (1)	LYG (1)
		GBM (17)	AE (1)	Metastatic tumor (2)
			AOA (2)	Craniopharyngioma (1)
			AO (8)	Hmartoma (1)
			GBMO (5)	Hemangioblastoma (1)
			Central neurocytoma (1)	Atypical meningioma (1)

Numbers in parentheses indicate the number of patients

DA diffuse astrocytoma, *AA* anaplastic astrocytoma, *GBM* glioblastoma multiforme, *OA* oligoastrocytoma, *OL* oligodendroglioma, *AE* anaplastic ependymoma, *AOA* anaplastic oligoastrocytoma, *AO* anaplastic oligodendroglioma, *GBMO* GBM with an oligodendroglial component, *PCNSL* primary central nervous system lymphoma, *LYG* lymphomatoid granulomatosis

visual assessment in all groups (groups 1, 2, and 3: $p < 0.00001$, $p < 0.001$, and $p < 0.01$, respectively).

The relationship between TNR and visual analysis

The means ± SD of the TNR for FMISO-positive and -negative uptake lesions were 3.56 ± 0.93 and 1.43 ± 0.24, respectively. The TNR of the FMISO-positive uptake group was significantly higher than that of the FMISO-negative group ($p < 0.00001$, Welch's t test). ROC analysis revealed a close correlation between TNR and visual analysis [area under the curve (AUC) = 0.998].

TNR and necrosis

The TNR in group 1 was 3.49 ± 0.97 vs. 1.43 ± 0.42 (with vs. without necrosis), the TNR in group 2 was 2.91 ± 0.83 vs. 1.44 ± 0.20, and the TNR in group 3 was 2.63 ± 1.16 vs. 1.35 ± 0.23 (Fig. 1). The TNRs of cases with necrosis were significantly higher than those of cases without necrosis in each group (group 1, 2, and 3: $p < 0.00001$, $p < 0.005$, and $p < 0.05$, respectively).

Semi-quantitative analysis

The mean + 3SD as the cut-off value was TNR = 1.67. When we divided the patients into two groups with high or low TNRs, the necrosis fraction was 1/28 (3.6 %) in the low TNR group and 29/31 (93.5 %) in the high TNR group (Fig. 2).

The ROC curve towards necrosis and TNR including all cases is shown in Fig. 3. The AUC was 0.990. At the cut-off value (TNR = 1.67), the sensitivity, specificity, and accuracy were 96.7, 93.1, and 94.9 %, respectively.

Illustrative case

One illustrative case with multifocal GBM was presented. The patient was an 80-year-old female presenting with motor dominant aphasia. MRI revealed two contrast-enhanced lesions in the left frontal lobe. These lesions showed different uptake patterns of FMISO PET. One lesion showed FMISO-positive uptake, whereas the other showed FMISO-negative uptake (Fig. 4a). Biopsies were performed to target each lesion. A specimen from the FMISO-positive lesion showed clear necrosis, whereas the specimen from the FMISO-negative lesion did not show necrosis (Fig. 4b).

Table 2 Interrater correlation for FMISO visual assessment

		Radiologist A		
		High	Intermediate	Low
Radiologist B	High	27	1	0
	Intermediate	0	1	1
	Low	0	3	26

Table 3 Existence probability of necrosis by FMISO visual assessment

	Group 1		Group 2		Group 3	
Necrosis	+	−	+	−	+	−
FMISO-positive uptake	17	1	5	0	4	0
FMISO-negative uptake	0	7	2	13	2	8

Fig. 1 Differences and distribution of FMISO TNRs in group 1, 2, 3, and all groups. The mean TNRs of cases with necrosis were 3.49 ± 0.97 in group 1, 2.91 ± 0.83 in group 2, and 2.63 ± 1.16 in group 3, which were significantly higher than those of cases without necrosis in each group (group 1, 2, and 3: $*p < 0.00001$, $^{\dagger}p < 0.005$, and $^{\S}p < 0.05$; Welch's t test)
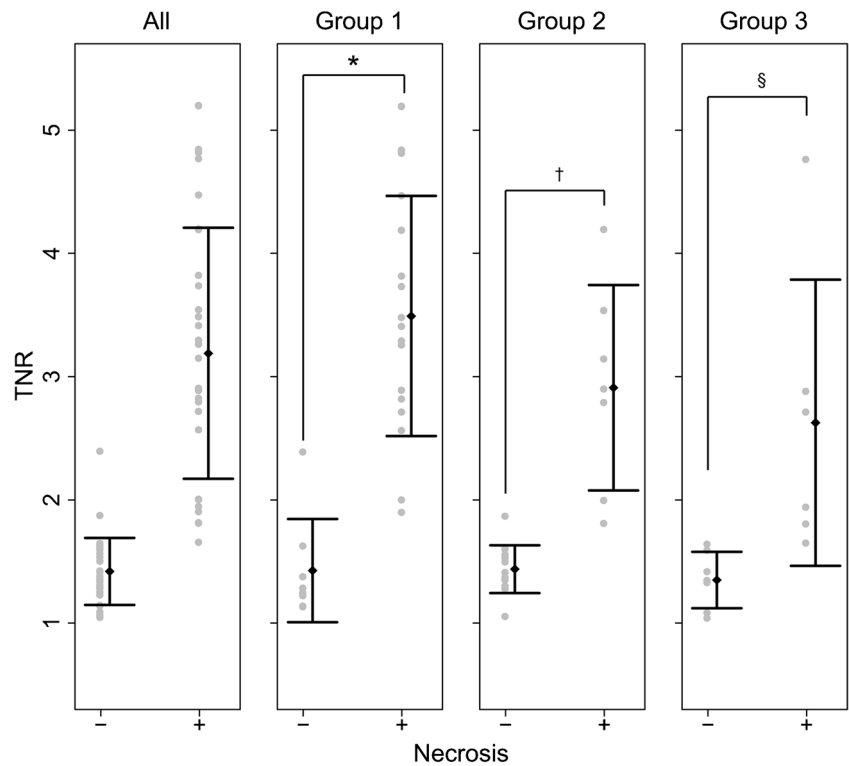
Discussion

In this study, both visual and semi-quantitative analyses indicated a strong correlation between the FMISO uptake status and the presence of necrosis. The correlations were significant not only in astrocytic tumors but also in various histological types of brain tumor. Our results suggest that FMISO PET can predict pathological necrosis regardless of the histopathological subtypes.
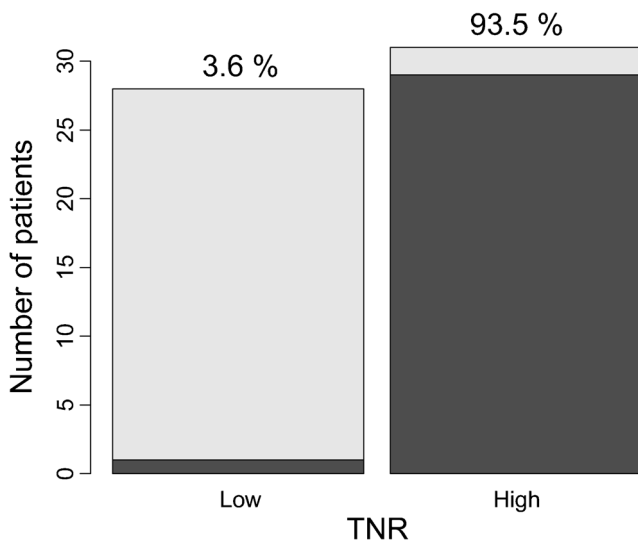
Fig. 2 Necrosis fractions in high TNR (≥ 1.67) and low TNR (< 1.67) groups. The *grey* area represents negative necrosis, and the *dark grey* area indicates positive necrosis. The necrosis fraction was 1/28 (3.6 %) in the low TNR group and 29/31 (93.5 %) in the high TNR group
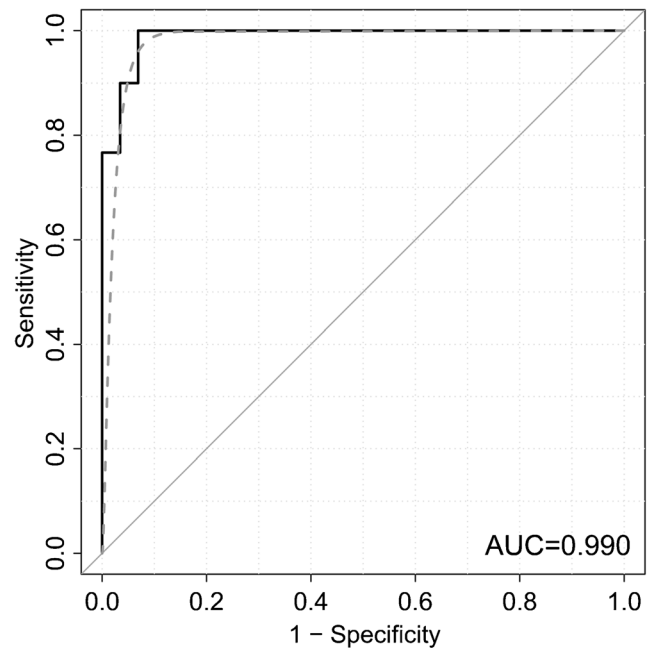
Fig. 3 ROC curve for the presence of necrosis generated from TNRs including all cases. The ROC curve showed a very good correlation between necrosis and TNR (AUC = 0.990). At the cut-off value (TNR = 1.67), the sensitivity, specificity, and accuracy were 96.7, 93.1, and 94.9 %, respectively
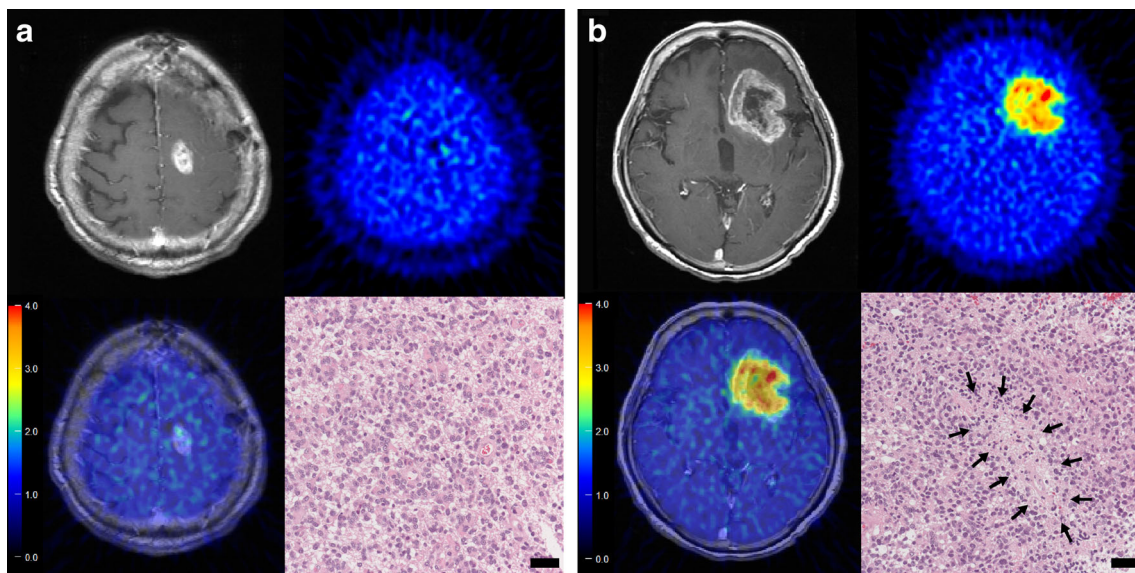
Fig. 4 Illustrative case with multifocal GBM. MRI revealed two contrast-enhanced lesions in the left frontal lobe. The upper lesion showed FMISO-negative uptake and a TNR of 1.62 (**a**). This specimen did not contain necrosis. The lower lesion showed FMISO-positive uptake and a TNR of 3.54 (**b**). This specimen had clearly observed necrosis. *Black bars* represent 50μm

It is well established that FMISO PET can image regional hypoxia. In addition, the mechanisms of FMISO uptake have been described previously [19]. Once FMISO is delivered to cells, retention of FMISO requires, as the first step, electron release from the electron transport chain into the cytosol where the electrons react with the electron-affinic nitro group. Thus, FMISO does not accumulate in necrotic cells itself but rather in peri-necrotic hypoxic cells. Essentially, as tumor cells proliferate, an insufficient oxygen supply may cause local hypoxia [20]. Even though malignant tumor cells are resistant to such severe circumstances, a fraction of cells would fail to survive and thus undergo necrosis [21]. It appears that both the presence of intratumoral micro-necrosis and FMISO uptake have certain thresholds of pO_2 pressure. Our results of strong agreement between necrosis and FMISO uptake suggest that the thresholds are close to each other.

A major result of this study was that FMISO PET could also visualize histologically detectable intratumoral micro-necrosis in vivo. So far, central necrosis is an important finding in malignant brain tumors, and wide-ranging necrosis can be clearly detected by conventional MRI. However, histological micro-necrosis is also important for the diagnosis of malignant brain tumors, especially GBM, because the presence of micro-necrosis is critical information for GBM diagnosis regardless of imaging central necrosis [2]. In addition, atypical and anaplastic meningiomas frequently have histopathological necrosis, and the patient outcomes of these tumors are usually poorer than those of ordinary meningiomas [1, 22].

In this context, FMISO-positive areas might indicate not only severe hypoxic areas (necrotic areas), but also malignant parts of the tumor. FMISO PET might be able to visualize the

tumor malignancy in many types of brain tumors. In fact, there are several lines of evidence showing that FMISO-positive lesions are associated with tumor malignancy. These studies indicated that a large volume of hypoxia in glioma measured by FMISO PET is strongly associated with a poorer prognosis [23–26].

Another application of FMISO PET in clinical practice is providing important information for biopsy. Brain tumors, especially gliomas, have histological heterogeneity. Therefore, FMISO may contribute to determining the biopsy site as well as accurate diagnosis of the histological malignancy of these tumors. In addition, FMISO uptake evaluation is reproducible and simple, thus providing valid information [27]. The visual evaluations of the two radiologists were very well correlated in the current study. In the illustrative case, intratumoral FMISO accumulation was heterogeneous within individual tumors, and the presence of necrosis corresponded with the FMISO uptake (Fig. 4).

FMISO PET can provide prognostic information immediately and non-invasively. Clinical symptoms often progress rapidly in brain tumor patients. In such cases, FMISO PET findings might be able to quickly provide information to evaluate necrosis as well as information for differential diagnosis. Furthermore, some cases would benefit from omission of biopsy based on FMISO PET examination, especially elderly patients or patients with severe complications.

Semi-quantitative analysis may be informative for evaluation of FMISO PET. When cases presented with equivocal FMISO accumulation, the visual evaluations by multiple radiologists did not always correspond. In this study, we defined these cases as FMISO negative. In contrast, semi-quantitative

analysis could more definitely evaluate these intermediate FMISO uptakes. TNR = 1.67 might be an adequate cut-off value for the prediction of necrosis. Therefore, we should consider the TNR when evaluating FMISO PET, especially in lesions that show equivocal FMISO uptake. In fact, there were four cases of exceptions in visual analysis. Two cases in group 2 and two cases in group 3 with necrosis-positive samples showing FMISO-negative uptake. One of the group 2 cases, which were diagnosed as AO, had a TNR of 2.00, and AE had a TNR of 1.81. Moreover, the two nuclear medicine physicians both evaluated the same area as intermediate or high. Therefore, FMISO uptake in this case may be a significant finding. On the other hand, two cases in group 3 diagnosed as PCNSL showed lower TNRs, and visual analysis did not indicate a matched area. We considered that there might be other mechanisms of necrosis induction in PCNSL.

The potential pitfall of the correlation between FMISO and necrosis may be treatment-induced necrotic changes resulting from steroids or other chemotherapeutic drugs administered before tumor sampling. Such changes may also affect pathological evaluation. To avoid this possibility, we excluded patients who underwent any treatments before FMISO PET and tumor sampling.

One of the limitations of this study was the small numbers of patients, especially in group 3. The tolerance to hypoxia might be different among histopathological features. We are also interested in evaluating protein expression, gene mutations, and any other differences between FMISO uptake-positive and -negative lesions. Further studies, especially of non-glioma patient populations, are necessary to verify our results and clarify the molecular fundamentals.

Conclusions

This study demonstrated a strong correlation between the presence of necrosis and FMISO uptake. Regardless of pathological subtypes, FMISO uptake within the lesion indicated the presence of necrosis. Our results suggest that FMISO PET could provide important information for treatment decisions and surgical strategies of any type of brain tumor.

References

1. Moradi A, Semnani V, Djam H, Tajodini A, Zali AR, Ghaemi K, et al. Pathodiagnostic parameters for meningioma grading. J Clin Neurosci: Off J Neurosurg Soc Aust. 2008;15(12):1370–5. doi:10.1016/j.jocn.2007.12.005.

2. Louis DN, Ohgaki H, Wiestler OD, Cavenee WK, Burger PC, Jouvet A, et al. The 2007 WHO classification of tumours of the central nervous system. Acta Neuropathol. 2007;114(2):97–109. doi:10.1007/s00401-007-0243-4.

3. Miller CR, Dunham CP, Scheithauer BW, Perry A. Significance of necrosis in grading of oligodendroglial neoplasms: a clinicopathologic and genetic study of newly diagnosed high-grade gliomas. J Clin Oncol: Off J Am Soc Clin Oncol. 2006;24(34):5419–26. doi:10.1200/JCO.2006.08.1497.

4. Lacroix M, Abi-Said D, Fourney DR, Gokaslan ZL, Shi W, DeMonte F, et al. A multivariate analysis of 416 patients with glioblastoma multiforme: prognosis, extent of resection, and survival. J Neurosurg. 2001;95(2):190–8. doi:10.3171/jns.2001.95.2.0190.

5. Urtasun R, Band P, Chapman JD, Feldstein ML, Mielke B, Fryer C. Radiation and high-dose metronidazole in supratentorial glioblastomas. N Engl J Med. 1976;294(25):1364–7. doi:10.1056/NEJM197606172942503.

6. Dische S. Chemical sensitizers for hypoxic cells: a decade of experience in clinical radiotherapy. Radiother Oncol: J Eur Soc Ther Radiol Oncol. 1985;3(2):97–115.

7. Van Os-Corby DJ, Koch CJ, Chapman JD. Is misonidazole binding to mouse tissues a measure of cellular pO2? Biochem Pharmacol. 1987;36(20):3487–94.

8. Rasey JS, Nelson NJ, Chin L, Evans ML, Grunbaum Z. Characteristics of the binding of labeled fluoromisonidazole in cells in vitro. Radiat Res. 1990;122(3):301–8.

9. Kavanagh MC, Sun A, Hu Q, Hill RP. Comparing techniques of measuring tumor hypoxia in different murine tumors: Eppendorf pO2 Histograph, [3H]misonidazole binding and paired survival assay. Radiat Res. 1996;145(4):491–500.

10. Piert M, Machulla H, Becker G, Stahlschmidt A, Patt M, Aldinger P, et al. Introducing fluorine-18 fluoromisonidazole positron emission tomography for the localisation and quantification of pig liver hypoxia. Eur J Nucl Med. 1999;26(2):95–109.

11. Piert M, Machulla HJ, Becker G, Aldinger P, Winter E, Bares R. Dependency of the [18F]fluoromisonidazole uptake on oxygen delivery and tissue oxygenation in the porcine liver. Nucl Med Biol. 2000;27(8):693–700.

12. Bentzen L, Keiding S, Horsman MR, Gronroos T, Hansen SB, Overgaard J. Assessment of hypoxia in experimental mice tumours by [18F]fluoromisonidazole PET and pO2 electrode measurements. Influence of tumour volume and carbogen breathing. Acta Oncol. 2002;41(3):304–12.

13. Hirata K, Terasaka S, Shiga T, Hattori N, Magota K, Kobayashi H, et al. (1)(8)F-Fluoromisonidazole positron emission tomography may differentiate glioblastoma multiforme from less malignant gliomas. Eur J Nucl Med Mol Imaging. 2012;39(5):760–70. doi:10.1007/s00259-011-2037-0.

14. Grunbaum Z, Freauff SJ, Krohn KA, Wilbur DS, Magee S, Rasey JS. Synthesis and characterization of congeners of misonidazole for imaging hypoxia. J Nucl Med: Off Publ Soc Nucl Med. 1987;28(1):68–75.

15. Thorwarth D, Eschmann SM, Paulsen F, Alber M. A kinetic model for dynamic [18F]-Fmiso PET data to analyse tumour hypoxia. Phys Med Biol. 2005;50(10):2209–24. doi:10.1088/0031-9155/50/10/002.

16. Wahl RL, Jacene H, Kasamon Y, Lodge MA. From RECIST to PERCIST: evolving considerations for PET response criteria in

solid tumors. J Nucl Med: Off Publ Soc Nucl Med. 2009;50 Suppl 1:122S–50. doi:10.2967/jnumed.108.057307.

17. Kobayashi K, Hirata K, Yamaguchi S, Manabe O, Terasaka S, Kobayashi H, et al. Prognostic value of volume-based measurements on (11)C-methionine PET in glioma patients. Eur J Nucl Med Mol Imaging. 2015;42(7):1071–80. doi:10.1007/s00259-015-3046-1.

18. Robin X, Turck N, Hainard A, Tiberti N, Lisacek F, Sanchez JC, et al. pROC: an open-source package for R and S+ to analyze and compare ROC curves. BMC Bioinforma. 2011;12:77. doi:10.1186/1471-2105-12-77.

19. Lee ST, Scott AM. Hypoxia positron emission tomography imaging with 18f-fluoromisonidazole. Semin Nucl Med. 2007;37(6):451–61. doi:10.1053/j.semnuclmed.2007.07.001.

20. Bell C, Dowson N, Fay M, Thomas P, Puttick S, Gal Y, et al. Hypoxia imaging in gliomas with 18F-fluoromisonidazole PET: toward clinical translation. Semin Nucl Med. 2015;45(2):136–50. doi:10.1053/j.semnuclmed.2014.10.001.

21. Jenkins WT, Evans SM, Koch CJ. Hypoxia and necrosis in rat 9L glioma and Morris 7777 hepatoma tumors: comparative measurements using EF5 binding and the Eppendorf needle electrode. Int J Radiat Oncol Biol Phys. 2000;46(4):1005–17.

22. Yamaguchi S, Terasaka S, Kobayashi H, Asaoka K, Motegi H, Nishihara H, et al. Prognostic factors for survival in patients with high-grade meningioma and recurrence-risk stratification for application of radiotherapy. PLoS One. 2014;9(5), e97108. doi:10.1371/journal.pone.0097108.

23. Szeto MD, Chakraborty G, Hadley J, Rockne R, Muzi M, Alvord Jr EC, et al. Quantitative metrics of net proliferation and invasion link biological aggressiveness assessed by MRI with hypoxia assessed by FMISO-PET in newly diagnosed glioblastomas. Cancer Res. 2009;69(10):4502–9. doi:10.1158/0008-5472.CAN-08-3884.

24. Spence AM, Muzi M, Swanson KR, O'Sullivan F, Rockhill JK, Rajendran JG, et al. Regional hypoxia in glioblastoma multiforme quantified with [18F]fluoromisonidazole positron emission tomography before radiotherapy: correlation with time to progression and survival. Clin Cancer Res: Off J Am Assoc Cancer Res. 2008;14(9): 2623–30. doi:10.1158/1078-0432.CCR-07-4995.

25. Swanson KR, Chakraborty G, Wang CH, Rockne R, Harpold HL, Muzi M, et al. Complementary but distinct roles for MRI and 18F-fluoromisonidazole PET in the assessment of human glioblastomas. J Nucl Med: Off Publ Soc Nucl Med. 2009;50(1):36–44. doi:10.2967/jnumed.108.055467.

26. Kawai N, Lin W, Cao WD, Ogawa D, Miyake K, Haba R, et al. Correlation between 18F-fluoromisonidazole PET and expression of HIF-1alpha and VEGF in newly diagnosed and recurrent malignant gliomas. Eur J Nucl Med Mol Imaging. 2014;41(10):1870–8. doi:10.1007/s00259-014-2776-9.

27. Okamoto S, Shiga T, Yasuda K, Ito YM, Magota K, Kasai K, et al. High reproducibility of tumor hypoxia evaluated by 18F-fluoromisonidazole PET for head and neck cancer. J Nucl Med: Off Publ Soc Nucl Med. 2013;54(2):201–7. doi:10.2967/jnumed.112.109330.